

# Computational fluid dynamics-based study of possibility of generating pulsatile blood flow via a continuous-flow VAD

Erfan Nammakie<sup>1</sup> · Hanieh Niroomand-Oscuii<sup>1</sup> · Mojtaba Koochaki<sup>1</sup> · Farzan Ghalichi<sup>1</sup>

Received: 28 September 2015 / Accepted: 11 May 2016 / Published online: 27 May 2016  
© International Federation for Medical and Biological Engineering 2016

**Abstract** Until recent years, it was almost beyond remedy to save the life of end-stage heart failure patients without considering a heart transplant. This is while the need for healthy organs has always far exceeded donations. However, the evolution of VAD technology has certainly changed the management of these patients. Today, blood pumps are designed either pulsatile flow or continuous flow, each of which has its own concerns and limitations. For instance, pulsatile pumps are mostly voluminous and hardly can be used for children. On the other hand, the flow generated by continuous-flow pumps is in contrast with pulsatile flow of the natural heart. In this project, having used computational fluid dynamics, we studied the possibility of generating pulsatile blood flow via a continuous-flow blood pump by adjusting the rotational speed of the pump with two distinct patterns (sinusoidal and trapezoidal), both of which have been proposed and set based on physiological needs and blood flow waveform of the natural heart. An important feature of this study is setting the outlet pressure of the pump similar to the physiological conditions of a patient with heart failure, and since these axial pumps are sensitive to outlet pressures, more secure and reliable results of their performance are achieved. Our results show a slight superiority of a sinusoidal pattern compared to a trapezoidal one with the potential to achieve an adequate pulsatile flow by precisely controlling the rotational speed.

**Keywords** Ventricular assist device · CFD · Pulsatile flow · Hemolysis

## 1 Introduction

Currently, heart diseases are among the leading causes of mortality around the world, especially in highly economical countries. Since 1960, for instance, heart failure has been the first cause of death in the USA [25]. Presently, various treatment programs are available for heart failure. However, due to fundamental drawbacks to organ transplantation, heart transplantation is counted as the last medical treatment to which cardiologists and surgeons refer. Although scientists are perpetually trying to tackle the problem by employing stem cells to grow organs, this outstanding endeavor fails to fulfill the emergency needs and, therefore, it seems that the only life-saving solution is the practice of ventricular assist devices (VADs) implantation [5, 18, 19, 26, 32]. VADs fall into two groups in terms of flow generation: pulsatile flow and continuous flow. Although most of VADs designed today are pulsatile, there is not a solid view on which is more appropriate. For instance, continuous-flow pumps are remarkably smaller than pulsatile-flow ones and, therefore, their implantation is much less burdensome [9, 30, 36]. On the other hand, pulsatility of blood flow decreases the risk of thrombus formation inside blood pumps [10, 28]. Several works debated over the advantages and disadvantages of pulsatile-flow versus continuous-flow pumps [22, 29, 33]. Shahraki et al. optimized the function of a bichamber VAD by investigating three driver patterns and produced pulsatile flow [31]. Kato et al. [17] evaluated the echocardiographic parameters of the left ventricular of 61 patients following implantation of continuous-flow and pulsatile-flow VADs. Their study revealed that the left ventricle functions were better in patients with pulsatile-flow VADs. In a study of 27 patients receiving

✉ Hanieh Niroomand-Oscuii  
niroomand@sut.ac.ir

<sup>1</sup> Division of Biomechanics, Department of Mechanical Engineering, Sahand University of Technology, Sahand New Town, Tabriz, Iran

VADs carried out by Feller et al., it was revealed that cardiopulmonary bypass time in continuous-flow VADs are shorter than in pulsatile types [12]. This is while having implanted 31 LVADs, Klotz et al. [20] demonstrated that the output flow rate generated by pulsatile LVADs is higher than those by continuous-flow types.

In this study, we focus our attention on an axial flow VAD by proposing two modulation speed patterns that may contribute to reduce the known complications of rotary blood pumps in a clinical setting and help with the design of a miniature pump easier to implant. In addition, the clinical application of this method may well achieve adequate blood flow rate control within a specific range according to patients' need. It is also worthwhile to mention that the study carried out by Agarwal et al. [1] demonstrates the comparability of the size of the proposed VAD with other newer generation VADs.

## 2 Materials and methods

Computational fluid dynamics (CFD) has been used for designing and optimizing blood pumps in recent years [6,

23, 37]. Applying ANSYS software as a powerful numerical package, we have optimized the outflow waveform of a blood pump.

### 2.1 Geometry of the pump

This magnetically levitated pump consists of four parts, namely inducer, impeller, diffuser, and straightener (Fig. 1).

The dimensions and characteristics of all parts of the pump are shown in Table 1.

### 2.2 Governing equations

The general and dimensionless forms of fluid governing equations are as follows:

$$\frac{\partial \rho^*}{\partial t} + \nabla^* \cdot \rho^* V^* = 0 \quad (1)$$

$$\rho^* \frac{DV^*}{Dt^*} = -\nabla^* p^* + \frac{1}{Re} \nabla^* \cdot \left[ \mu^* \left( \frac{\partial u_i^*}{\partial x_j^*} + \frac{\partial u_j^*}{\partial x_i^*} \right) \right] \quad (2)$$

**Fig. 1** Geometry of the pump: **a** inducer; **b** impeller; **c** diffuser; **d** straightener

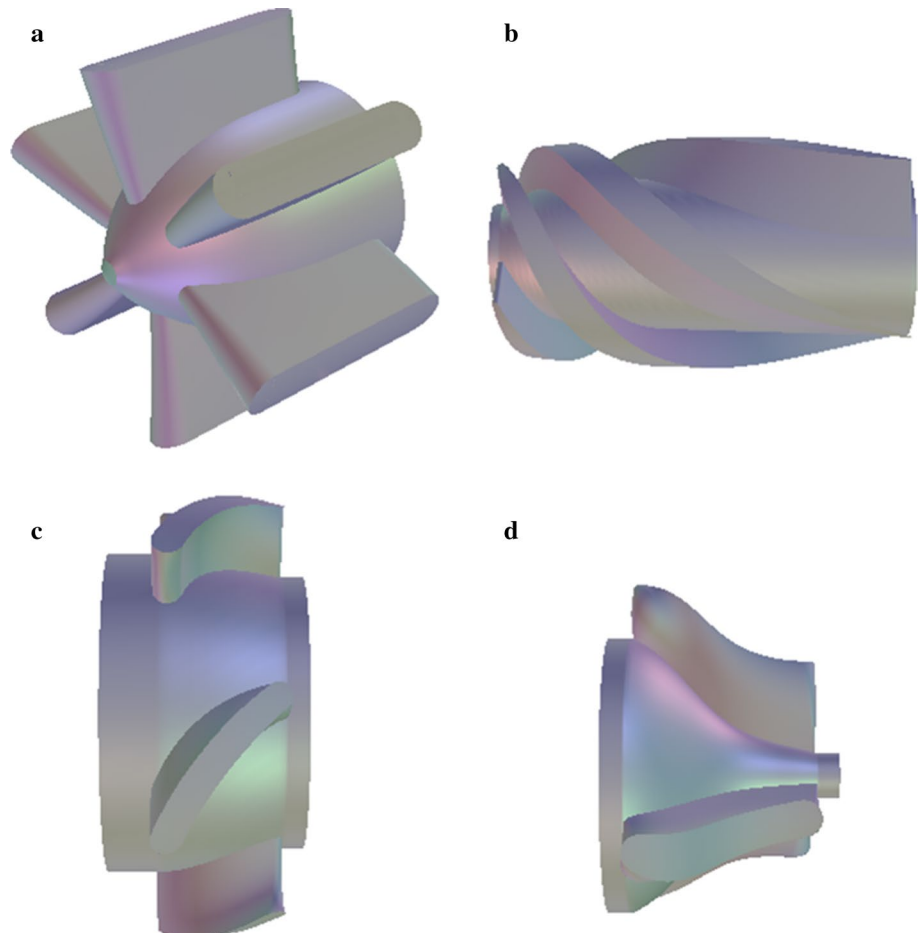


**Table 1** Dimensions and characteristics of all parts of the pump

	Inducer	Impeller	Diffuser	Straightener
Number of blades	6	4	5	3
Maximum thickness of blades (mm)	1.5	2.6	1.3	0.5
Length of the section (mm)	12.0	34.0	7.5	9.0
Average height of the blades (mm)	5.0	4.0	3.0	3.5
<i>General characteristics of the pump</i>				
Length of the pump (mm)	65			
Diameter of the pump (mm)	41			
Rotational speed (rpm)	3700–7500			
Inlet diameter of the pump (mm)	14			
Outlet diameter of the pump (mm)	10			

In these equations, the asterisk indicates that these parameters are dimensionless, while *Re* is the Reynolds number defined as follows [35]:

$$Re = \frac{\rho\omega D^2}{\mu} \tag{3}$$

where  $\rho$  is the density of the blood (1050 kg/m<sup>3</sup>),  $\mu$  is the viscosity of the blood (0.0035 Pa s),  $\omega$  is the rotational speed of the pump impeller (rad/s), and  $D$  is the diameter of the impeller (mm). It should be noted that when the Reynolds number exceeds 1.0E+04 in an axial flow blood pump, the flow is considered turbulent [34]. Here in this simulation, given the diameter and rotational speed of the pump, the Reynolds number is higher than the critical value, and, therefore, flow becomes turbulent. The *k*– $\epsilon$  turbulent model has been chosen for solving the turbulent flow equations whose nonlinear terms are calculated by semiempirical equations [2].

In axial rotary pumps, due to high rotational speed and the narrow clearance between rotary and stationary parts of the pump, slightly excessive amounts of shear stress are generated. On the other hand, the hemolysis index, defined

as the amount of the free hemoglobin concentration in the blood, is a function of both shear stress and the exposure time of the red blood cell (RBC) to the shear stress.

In 1980, Heuser [16] presented a power-law model for hemolysis expressing the relation between shear stress, exposure time, and the hemolysis index as follows:

$$\Delta HI = \frac{\Delta Hb}{Hb} = \left(1.8 \times 10^{-6} \tau^{1.991} \Delta t^{0.765}\right) \tag{4}$$

where  $\Delta Hb$  is the amount of free hemoglobin of the blood,  $Hb$  is the total amount of hemoglobin of the blood,  $\tau$  is the shear stress, and  $t$  is the exposure time.

The Lagrangian method is used to calculate the hemolysis index in blood pumps. In this approach, the instant measurements of shear stress and exposure time are followed by the integration of hemolysis index along a path line from which the amount of hemolysis is calculated:

$$HI(\%) = \left(\int_{t_0}^t 1.8 \times 10^{-6} \tau^{1.991} dt^{0.765}\right) \times 100 \tag{5}$$

where *HI* is the hemolysis index.

By taking the average over a sufficiently high number of streamlines, it is feasible to estimate the hemoglobin release (hemolysis percentage) in the blood pump. This method has been used by sundry persons such as Apel [3], Chan [8], Yano [38], and Arora [4].

### 2.3 Grid generation

For grid generation of different sections of the pump, TurboGrid software is manipulated, which is the special software for grid generation in turbomachines. The number of the elements for each section is shown in Table 2; this number for the impeller section is significantly higher than in the other parts for two major reasons: the considerable complexity of the geometry of the impeller’s blades and, the necessity for reaching the highest possible accuracy due to the fact that the impeller is the only rotational part of the pump and, therefore, the maximum amounts of the shear stress occur in this section.

It should be noted that a number of elements have been obtained following mesh independency calculations during

**Table 2** Number of elements of the pump

	Number of elements	Number of blades	Total number of elements of the section
Inducer	87,010	6	522,060
Impeller	292,688	4	1,170,752
Diffuser	103,560	5	517,800
Straightener	97,526	3	292,578
Total	–	–	2,503,190

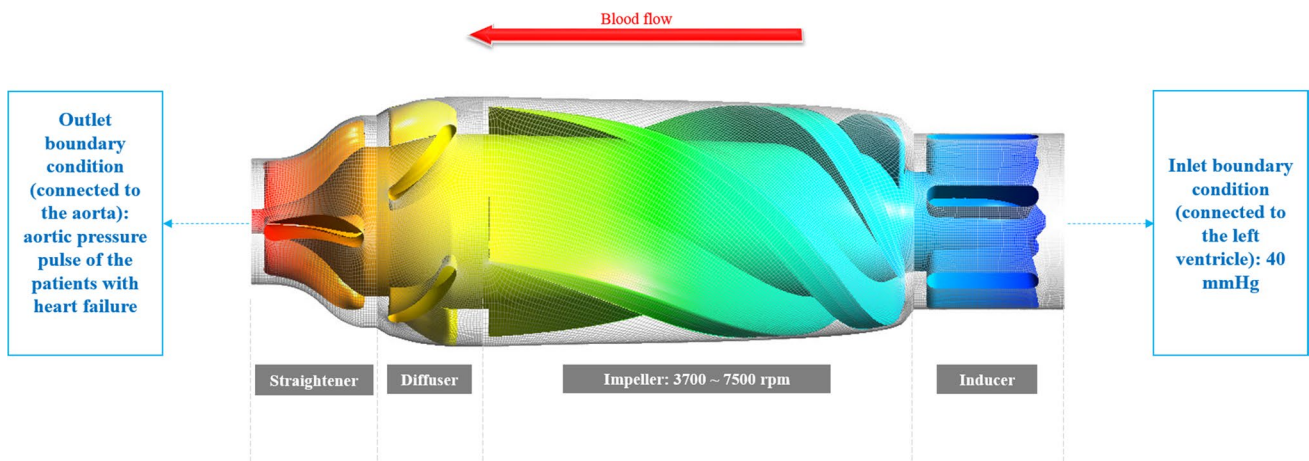


**Fig. 2** Various parts of the pump including the inlet and the outlet of the pump

which the effect of increasing the number of elements on two determinable factors, namely shear stress and flow rate, is studied.

#### 2.4 Boundary condition

In order for accurate determination of flow rate of the pump with variable rotational speed, pressure–pressure boundary conditions have been chosen for the inlet and outlet of the pump which equals 40 mmHg and aortic pressure pulse of the patients with heart failure, respectively. This is because the physiological pressures of the inlet and outlet of the pump are definite. The various parts of the pump including the inlet and the outlet of the pump (where the boundary conditions are defined) are shown in Fig. 2.

A healthy heart increases the blood pressure and provides the sufficient blood flow rate (which is approximately 6 l/min in normal adults) needed for the body. This is while in patients with heart failure, the heart is unable to provide adequate blood flow rate [21]. A comparison of aortic pressure pulse of a healthy heart with a heart failure has been depicted in Fig. 3.

Figure 3 demonstrates that the pulse generated by a heart failure is obviously weaker than that of a healthy heart and, therefore, adequate flow rate is supplemented in these patients and is carried out by implanting ventricular assist devices. However, the functional mechanism of these devices is completely antithetical to that of natural hearts. This means that in a natural heart, the flow rate is generated by the dramatic increase in pressure, while in VADs, high rotational speed of the impeller generates the sufficient flow rate. Furthermore, since the function of axial pumps are sensitive to the outlet pressure of the pump, more precise results could be achieved by applying physiological pressures to the outlet of the pump.

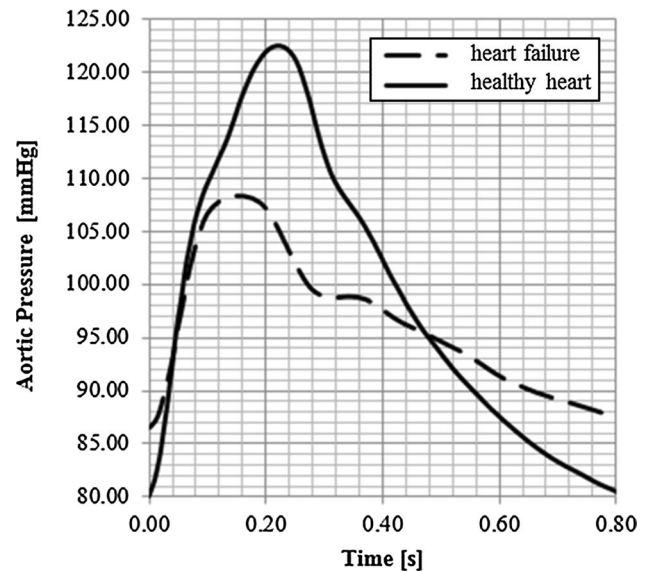


**Fig. 3** Comparison of aortic pressure pulse of a healthy heart with a heart failure [21]

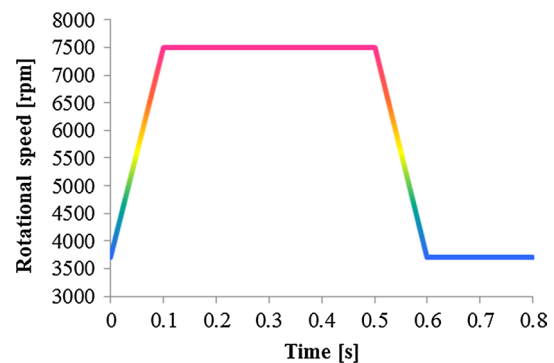


**Fig. 4** Trapezoidal pattern of variation in rotational speed

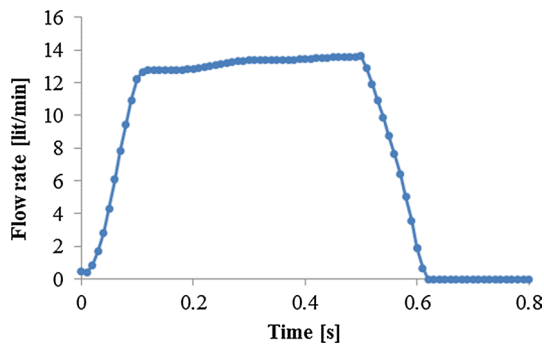


**Fig. 5** Numerically calculated flow rate versus time in trapezoidal cycle

### 2.5 Initial condition

This study aimed at evaluating the performance of a blood pump during a cardiac cycle by applying time-dependent rotational velocity to the impeller and, therefore, in addition to boundary conditions, the initial condition should also be set using time-independent solution. Since it is intended to achieve a very low amount of flow rate at the beginning of the cycle, an initial rotational velocity of 3500 rpm, necessary for prevention of reverse flow occurrence due to pressure gradient, was chosen for the impeller from which 0.46 l/min flow rate is produced.

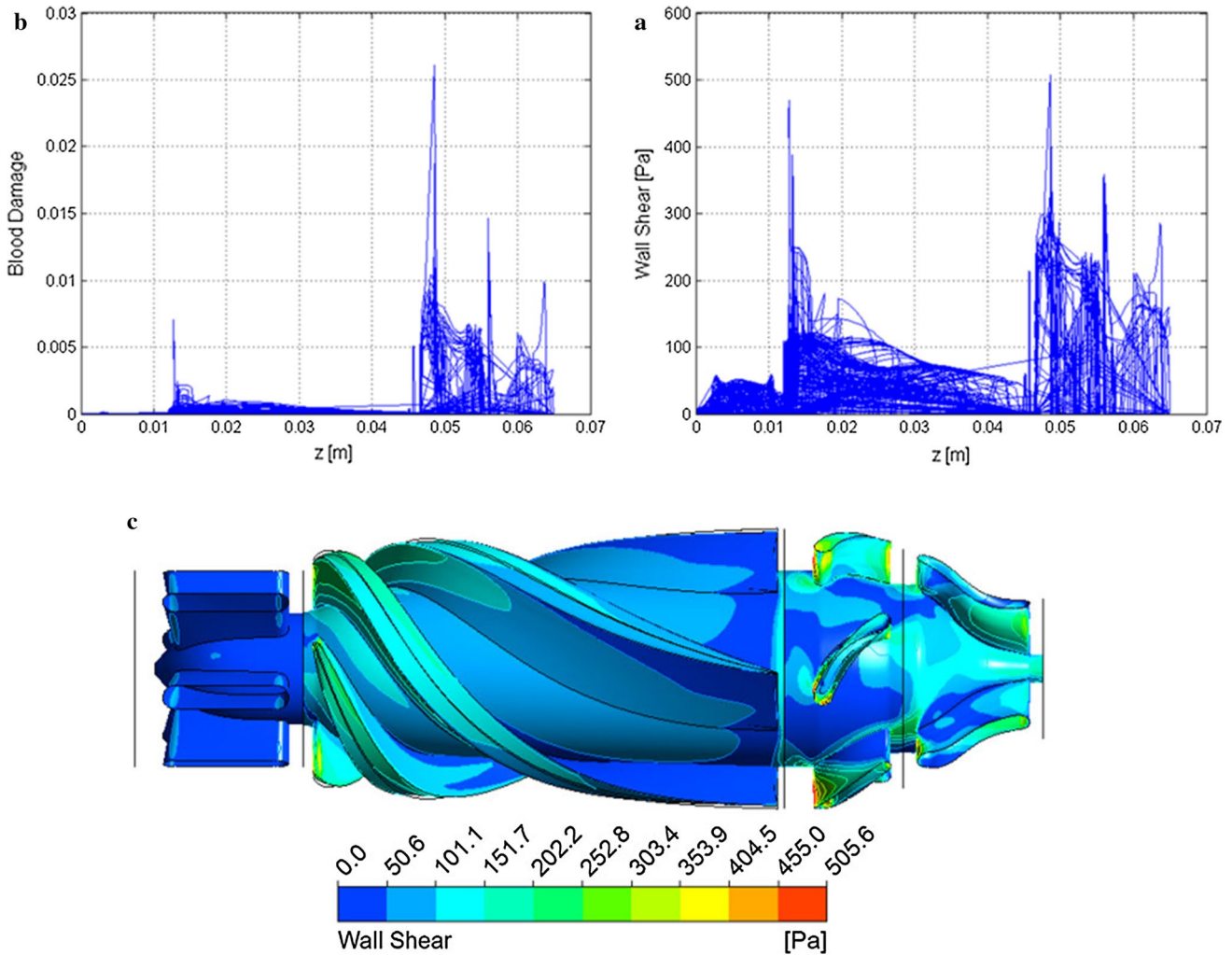


**Fig. 6** **a** Shear stress distribution; **b** hemolysis distribution; **c** contour diagram of shear stress distribution for trapezoidal cycle running at  $t = 0.1$  s

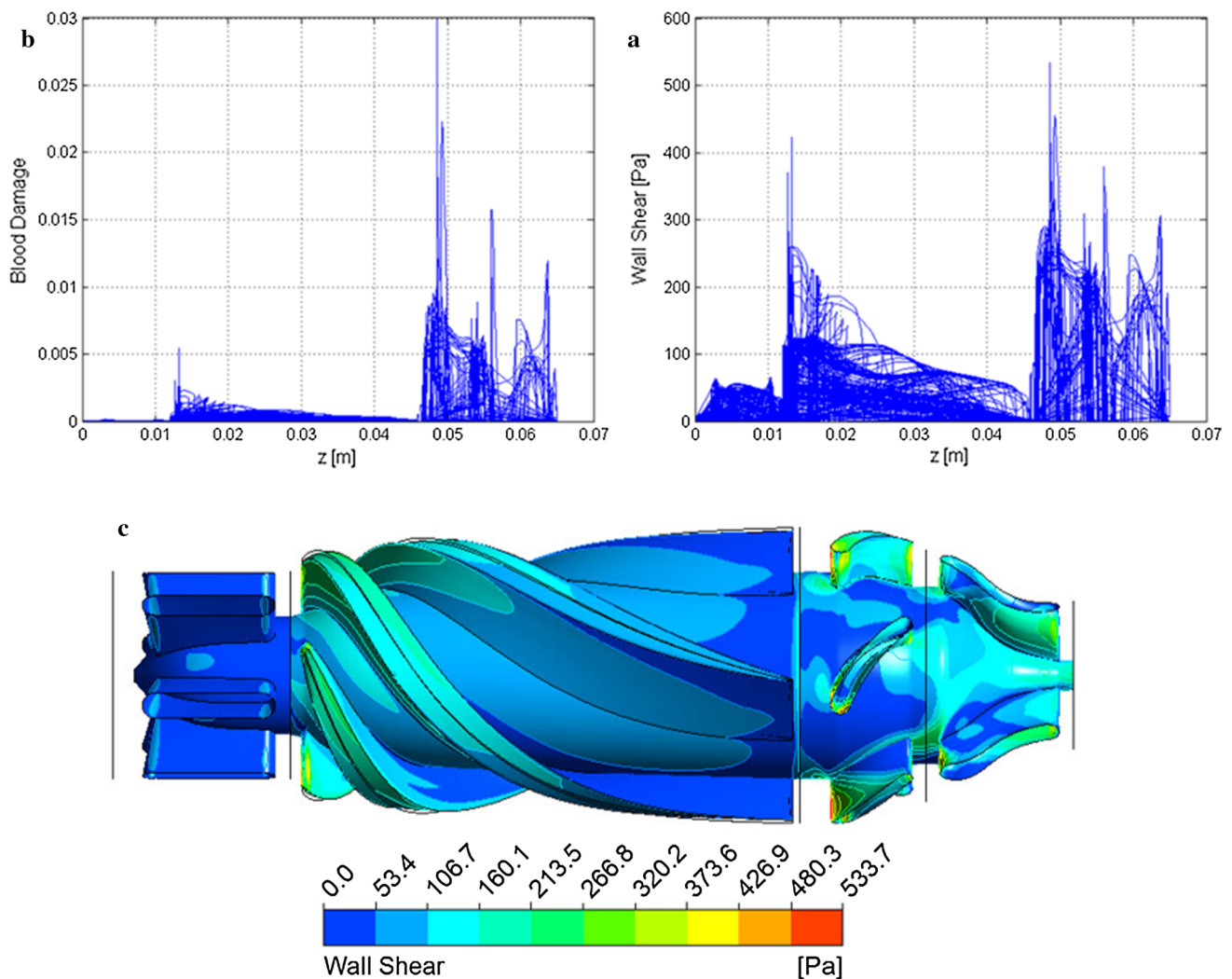


**Fig. 7** **a** Shear stress distribution; **b** hemolysis distribution; **c** contour diagram of shear stress distribution for trapezoidal cycle running at  $t = 0.15$  s

### 3 Results

In this project, the feasibility of simulating pulsatile flow of natural heart via continuous-flow blood pumps was studied. For this purpose, the performances of two different proposed patterns of rotational velocity for producing adequate amounts of flow rates, causing the least blood damages, were studied. It should be noted that a normal heart in adults produces approximately 6 l/min flow rate in every single cycle. Therefore, velocity should be set to generate an adequate flow rate with an appropriate flow waveform while less blood injuries occur inside the pump.

Trapezoidal pattern of variation in rotational speed, which is depicted in Fig. 4, consists of four phases: increasing the velocity ( $t = 0.0$  to  $t = 0.1$  s), maintaining the velocity at maximum value (0.1–0.5 s), reducing the

velocity ( $t = 0.5$  to  $t = 0.6$  s), and maintaining the velocity at a minimum value (0.6–0.8 s).

Owing to a need for understanding the total amount of generated flow rate within a cycle, Fig. 5 shows the graph of numerically calculated flow rate versus time in a trapezoidal cardiac cycle.

The following graphs (Figs. 6, 7) were plotted for hemolysis and shear stress distribution for 250 streamlines running at  $t = 0.1$  s and 0.15 s within the first and the second phases of trapezoidal cycle, respectively.

It is also feasible to study pressure distribution inside the pump running at  $t = 0.15$ , 0.4, and 0.6 s thanks to depiction of Fig. 8.

Sinusoidal pattern of variation in rotational speed is depicted in Fig. 9. In this pattern, the rotational velocity of the impeller varies sinusoidally in such a way that the

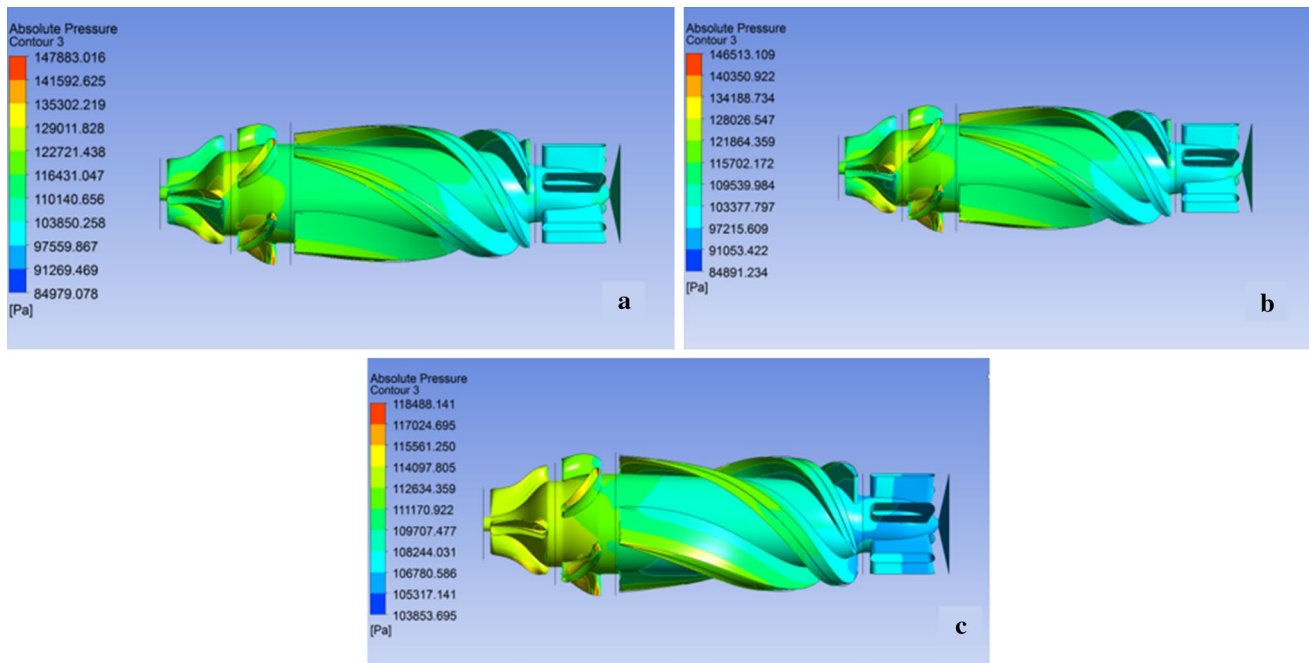


**Fig. 8** Pressure distribution for trapezoidal cycle running at **a**  $t = 0.15$  s; **b**  $t = 0.4$  s; **c**  $t = 0.6$  s

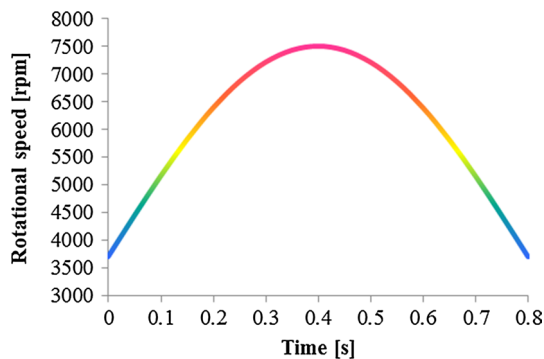


**Fig. 9** Sinusoidal pattern of variation in rotational speed

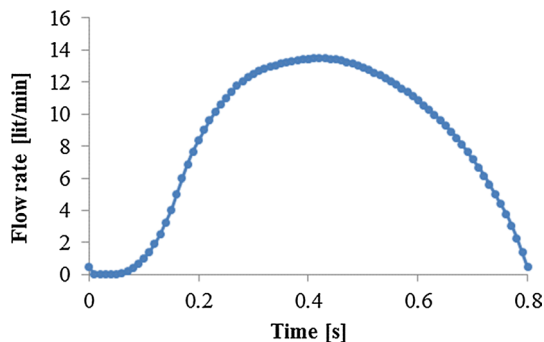


**Fig. 10** Numerically calculated flow rate versus time in sinusoidal cycle

minimum and maximum values are 3700 and 7500 rpm, respectively, and the performance of the pump during one cardiac cycle (0.8 s) is studied.

Figure 10 shows the graph of flow rate versus time for sinusoidal pattern.

Pressure distribution inside the pump at  $t = 0.4$  and  $t = 0.8$  s is shown in Fig. 11.

The results of instant calculation of hemolysis percentage during one cycle are shown in Fig. 12.

## 4 Discussion

The analysis of our results shows that the choice of pattern for the rotational speed of the impeller does affect the waveform of the generated flow rate. The advantages and disadvantages of each pattern will be discussed in the following paragraphs.

### 4.1 Trapezoidal pattern

This pattern, depicted in Fig. 3, is based on the pattern of aortic pulse and is designed in such a way that it is able to produce a minimum amount of 6 l/min in each cardiac cycle.

Accordingly, the reason for choosing 3700 rpm as the minimum initial velocity is to reach a value by which the generated flow rate at the beginning of the cycle is almost equal to zero, which is similar to the natural cardiac cycle.

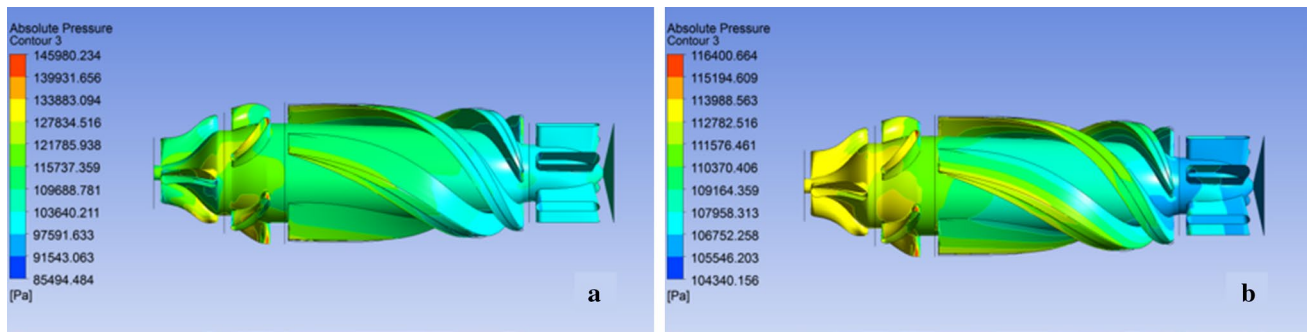


**Fig. 11** Pressure distribution for sinusoidal cycle running at **a**  $t = 0.4$  s; **b**  $t = 0.8$  s

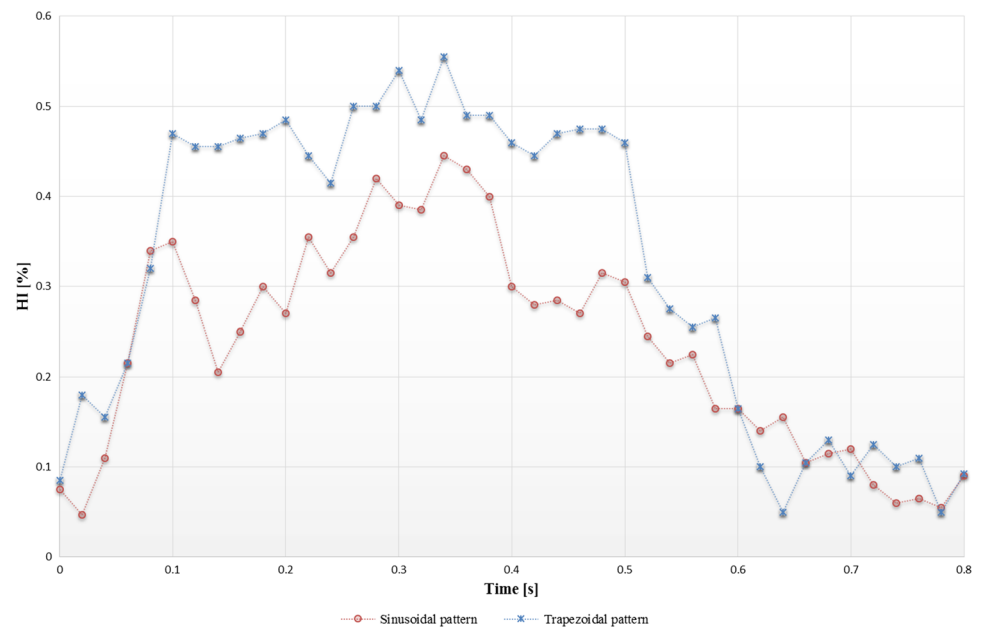
Furthermore, unlike the rotational velocity of the pump, the flow rate has slight fluctuations in the second phase due to pressure fluctuations.

The area under the calculated flow rate versus time in a trapezoidal cardiac cycle curve, depicted in Fig. 5, gives the total amount of flow rate in a single cycle which equals 6.65 l/min. This value is very close to the flow rate produced by a natural heart.

Hemolysis analysis at  $t = 0.1$  s (Fig. 6) shows that hemolysis index (the percentage of free hemoglobin in plasma to the total hemoglobin of blood) is 0.47 % and, therefore, the pump could work in an acceptable margin of safety.

Likewise, hemolysis index at  $t = 0.15$  s of the second phase of the cycle (Fig. 7), where aortic pressure pulse reaches its maximum, equals 0.46 %, indicating that the operation of the pump in this phase is innocuous. It should be pointed out that although the maximum shear stresses are relatively high at this moment, and since the exposure time is very short, blood cells are not detrimentally affected.

**Fig. 12** Instant measurement of hemolysis index in trapezoidal and sinusoidal cycles



In addition to this, pressure distribution inside the pump, depicted in Fig. 8, shows that the minimum pressure occurring inside the pump (849,891 Pa) is much higher than the vapor pressure of the blood and, therefore, cavitation does not occur inside the pump. The absolute vapor pressure of the blood under physiological conditions equals 47 mmHg (6266 Pa) [11].

#### 4.2 Sinusoidal pattern

This pattern (Fig. 9) is proposed based on the idea that in the former pattern, the pump operates at very low speeds and there is the probability of occurrence of stagnation points and reverse flow due to high fluctuation of aortic pressure.

The graph of flow rate versus time (Fig. 10) proves the nonlinearity of relationship between pressure gradient, rotational speed, and flow rate of the pump. According to this graph, it can be said that the performance of the pump



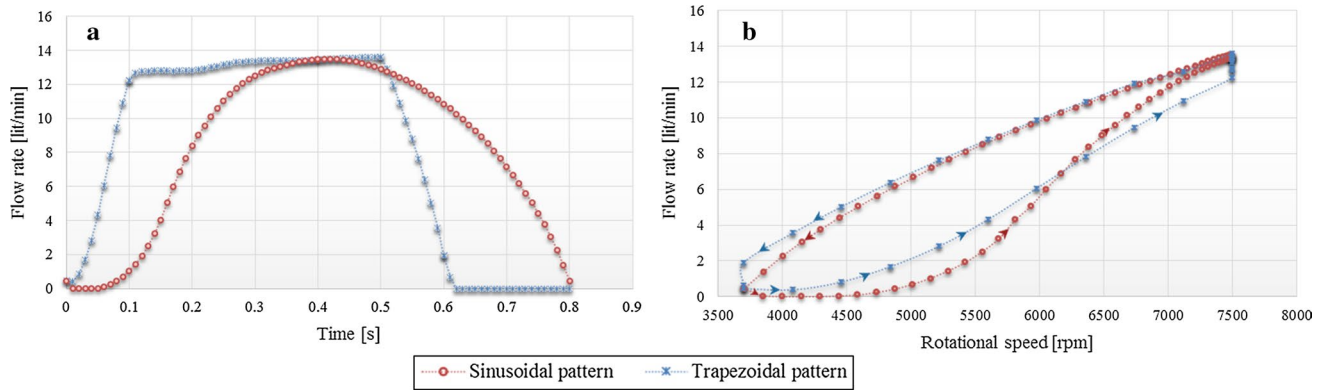


**Fig. 13** Resultant flow rates of trapezoidal and sinusoidal patterns **a** versus time; **b** versus rotational speed

also varies from ascending to descending pressure gradients, i.e., flow rate is in good agreement with the descending phase of pressure gradient while for the ascending phase, there exists a noticeable delay for the flow rate to be adapted with the pressure gradient. The total amount of flow rate in a single cycle equals 6.72 l/min.

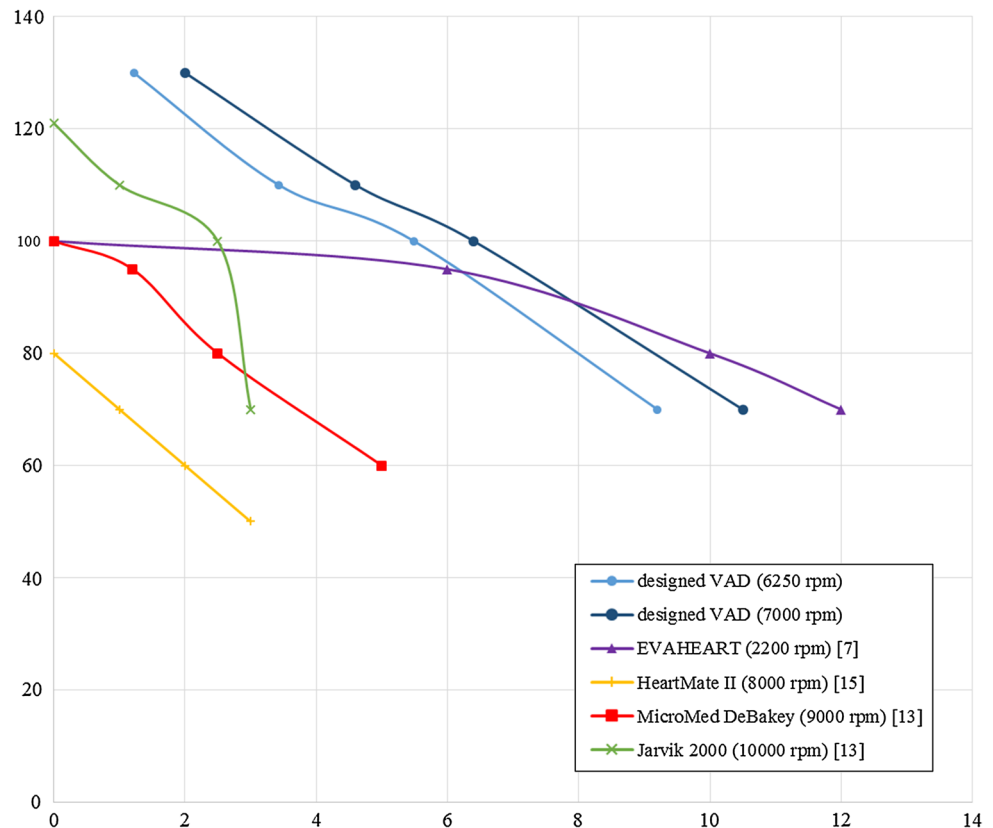
It should also be noted that pressure distribution inside the pump (Fig. 11) indicates that since the minimum pressure inside the pump (85494 Pa) is higher than the vapor pressure of the blood [11], cavitation does not occur in this cycle.

Furthermore, Fig. 12 indicates that the maximum amount for hemolysis index occurs at  $t = 0.34$  s which equals 0.44 %. This value is negligible and shows that RBCs traveling along streamlines are not likely to be ruptured.

### 4.3 Comparison of the patterns

To generate pulsatile flow, two distinct patterns for adjusting rotational speed of the pump have been proposed. As mentioned previously, the generated flow rate in both

**Fig. 14** Comparison of performance curve of the designed VAD with number of newer generation VADs [7, 13, 15]



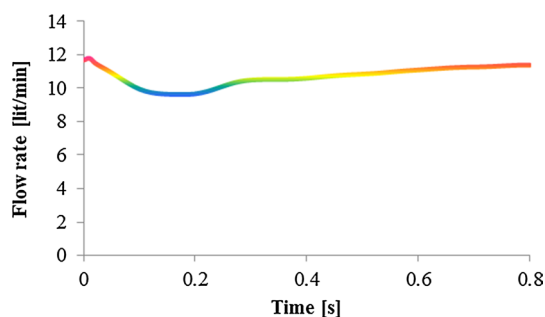


**Fig. 15** Variations of the output flow of the pump produced by a constant rotational speed running at 6500 rpm

cycles is sufficient and very close to that of a natural heart. In the trapezoidal cycle, because of the relatively long interval during which the output flow rate of the pump is almost zero, simulating the natural pulsatile flow of the heart is properly carried out; this is while the bare minimum of the output flow rate of the pump in this interval increases the probability of thrombus formation due to stagnation points and reverse flows (although the exposure time of blood inside the pump is much shorter than the time needed for platelets augmentation). Figure 13 compares the resultant flow rates of both patterns.

In order for better drawing a comparison of the designed VAD with the other commercial ones, its performance curve (pressure vs. flow rate for two different constant rotational speeds) together with number of newer generation VADs is depicted in Fig. 14.

The findings indicate that although a constant rotational speed could create fluctuation in output flow rate, this kind of fluctuation is in sharp contrast to the natural pulsatility of the heart and, therefore, not an adequate one. The variations of the output flow of the pump produced by a constant rotational speed and pulsatile outlet pressure are shown in Fig. 15.

Instant measurement of hemolysis index in both patterns is depicted in Fig. 12. The percentage of hemolysis index in trapezoidal pattern is higher than in sinusoidal pattern in almost the entire duration of the cycles. Furthermore, there is a noticeable similarity between hemolysis index variations versus time with rotational speeds. This is because of the fact that hemolysis is affected by shear stress which is proportional to the rotational speed.

## 5 Conclusion

According to the discussion, the authors believe in balance that the sinusoidal pattern of variation of rotational speed for the impeller of the pump is more promising and is preferred to the trapezoidal pattern. Moreover, with an

appropriate control of the pump speed through a determined pattern, it is feasible to generate a decent pulsatile flow without any functional defects.

Furthermore, it should be noted that the idea of generating pulsatile flow by continuous-flow pumps has been under debate in recent years [24, 27]. We have also studied the possibility of generating this kind of flow by proposing two specific patterns without claiming to propound a novel idea for generating pulsatile flow. Although blood damage measurement was carried out with military precision here, we still believe that as in the study by Hayward et al. [14], conducting a major review of decisive factors such as left ventricle suction, right ventricular failure, and blood pressure of the patient needs to be the subject of further scrutiny.

**Acknowledgments** The authors would like to acknowledge the help of the members of Computational Biomechanical Laboratory of Sahand University of Technology for their collaboration and without them the project would not be possible.

### Compliance with ethical standards

**Conflict of interest** The authors declare that they have no conflict of interest.

## References

1. Agarwal S, High KM (2012) Newer-generation ventricular assist devices. *Best Pract Res Clin Anaesthesiol* 26:117–130
2. ANSYS CFX-solver theory guide (2009) ANSYS, Inc., Canonsburg, PA
3. Apel J, Paul R, Klaus S, Siess T, Reul H (2001) Assessment of hemolysis related quantities in a microaxial blood pump by computational fluid dynamics. *Artif Organs* 25:341–347
4. Arora D, Behr M, Pasquali M (2006) Hemolysis estimation in a centrifugal blood pump using a tensor-based measure. *Artif Organs* 30:539–547
5. Boyle AJ, Ascheim DD, Russo MJ, Kormos RL, John R, Naka Y, Gelijns AC, Hong KN, Teuteberg JJ (2011) Clinical outcomes for continuous-flow left ventricular assist device patients stratified by pre-operative INTERMACS classification. *J Heart Lung Transplant* 30:402–407
6. Burgreen GW, Antaki JF, Griffith BP (1996) A design improvement strategy for axial blood pumps using computational fluid dynamics. *ASAIO J* 42:M354–M359
7. Centrigugal LVAS (2016). Evaheart Inc., Houston, TX
8. Chan W, Wong Y, Ding Y, Chua L, Yu S (2002) Numerical investigation of the effect of blade geometry on blood trauma in a centrifugal blood pump. *Artif Organs* 26:785–793
9. Cheng A, Williamitis CA, Slaughter MS (2014) Comparison of continuous-flow and pulsatile-flow left ventricular assist devices: is there an advantage to pulsatility? *Ann Cardiothorac Surg* 3:573
10. Corbett SC, Ajdari A, Coskun AU, Nayeb-Hashemi H (2010) Effect of pulsatile blood flow on thrombosis potential with a step wall transition. *ASAIO J* 56:290–295
11. Dexter EU, Aluri S, Radcliffe RR, Zhu H, Carlson DD, Heilman TE, Chandran KB, Richenbacher WE (1999) In vivo

- demonstration of cavitation potential of a mechanical heart valve. *ASAIO J* 45:436–441
12. Feller ED, Sorensen EN, Haddad M, Pierson RN, Johnson FL, Brown JM, Griffith BP (2007) Clinical outcomes are similar in pulsatile and nonpulsatile left ventricular assist device recipients. *Ann Thorac Surg* 83:1082–1088
  13. Frazier O, Khalil HA, Benkowski RJ, Cohn WE (2010) Optimization of axial-pump pressure sensitivity for a continuous-flow total artificial heart. *J Heart Lung Transplant* 29:687–691
  14. Hayward CS, Salamonsen R, Keogh AM, Woodard J, Ayre P, Prichard R, Walker R, Kotlyar E, Macdonald PS, Jansz P (2011) Effect of alteration in pump speed on pump output and left ventricular filling with continuous-flow left ventricular assist device. *ASAIO J* 57:495–500
  15. HeartMate I (2012) LVAS operating manual. Thoratec Corporation, Pleasanton, CA, 171:e7
  16. Heuser G, Opitz R (1980) A Couette viscometer for short time shearing of blood. *Biorheology* 17:17
  17. Kato TS, Chokshi A, Singh P, Khawaja T, Cheema F, Akashi H, Shahzad K, Iwata S, Homma S, Takayama H (2011) Effects of continuous-versus pulsatile-flow left ventricular assist devices on myocardial unloading and remodeling. *Circ Heart Fail* 4:546
  18. Kirklin JK, Naftel DC, Pagani FD, Kormos RL, Stevenson L, Miller M, Young JB (2012) Long-term mechanical circulatory support (destination therapy): on track to compete with heart transplantation? *J Thorac Cardiovasc Surg* 144:584–603
  19. Kirklin JK, Naftel DC, Kormos RL, Stevenson LW, Pagani FD, Miller MA, Baldwin JT, Young JB (2013) Fifth INTERMACS annual report: risk factor analysis from more than 6,000 mechanical circulatory support patients. *J Heart Lung Transplant* 32:141–156
  20. Klotz S, Deng MC, Stypmann J, Roetker J, Wilhelm MJ, Hammel D, Scheld HH, Schmid C (2004) Left ventricular pressure and volume unloading during pulsatile versus nonpulsatile left ventricular assist device support. *Ann Thorac Surg* 77:143–149
  21. Laskey W, Kussmaul W (1987) Arterial wave reflection in heart failure. *Circulation* 75:711–722
  22. Margulies KB, Rame JE (2011) Adaptations to pulsatile versus nonpulsatile ventricular assist device support. *Circ Heart Fail* 4:535–537
  23. Miyazoe Y, Sawairi T, Ito K, Konishi Y, Yamane T, Nishida M, Asztalos B, Masuzawa T, Tsukiya T, Endo S, Taenaka Y (1999) Computational fluid dynamics to establish the design process of a centrifugal blood pump: second report. *Artif Organs* 23:762–768
  24. Moazami N, Dembitsky W, Adamson R, Steffen R, Soltesz E, Starling R, Fukamachi K (2015) Does pulsatility matter in the era of continuous-flow blood pumps? *J Heart Lung Transplant* 34:999–1004
  25. Murphy SL, Xu J, Kochanek KD (2013) Deaths: final data for 2010. *Natl Vital Stat Rep* 61:1–118
  26. Park SJ, Tector A, Piccioni W, Raines E, Gelijns A, Moskowitz A, Rose E, Holman W, Furukawa S, Frazier OH (2005) Left ventricular assist devices as destination therapy: a new look at survival. *J Thorac Cardiovasc Surg* 129:9–17
  27. Pirbodaghi T, Axiak S, Weber A, Gempp T, Vandenberghe S (2012) Pulsatile control of rotary blood pumps: does the modulation waveform matter? *J Thorac Cardiovasc Surg* 144:970–977
  28. Prosi M, Perktold K, Schima H (2007) Effect of continuous arterial blood flow in patients with rotary cardiac assist device on the washout of a stenosis wake in the carotid bifurcation: a computer simulation study. *J Biomech* 40:2236–2243
  29. Sansone F, Zingarelli E, Flocco R, Dato GMA, Parisi F, Punta G, Forsennati PG, Bardi GL, del Ponte S, Patanè F (2012) Pulsed or continuous flow in long-term assist devices: a debated topic. *Transplant Rev* 26:241–245
  30. Schmid C, Tjan TD, Etz C, Schmidt C, Wenzelburger F, Wilhelm M, Rothenburger M, Drees G, Scheld HH (2005) First clinical experience with the Incor left ventricular assist device. *J Heart Lung Transplant* 24:1188–1194
  31. Shahraki ZH, Oscui HN (2014) Numerical investigation of three patterns of motion in an electromagnetic pulsatile VAD. *ASAIO J* 60:304–310
  32. Slaughter MS, Rogers JG, Milano CA, Russell SD, Conte JV, Feldman D, Sun B, Tatroles AJ, Delgado RM III, Long JW (2009) Advanced heart failure treated with continuous-flow left ventricular assist device. *N Engl J Med* 361:2241–2251
  33. Soucy KG, Koenig SC, Giridharan GA, Sobieski MA, Slaughter MS (2013) Rotary pumps and diminished pulsatility: do we need a pulse? *ASAIO J* 59:355–366
  34. Untaroiu A (2006) LEV-VAD2 Axial Flow blood pump optimized flow path design by means of computational fluid dynamics. University of Virginia, USA
  35. White FM, Corfield I (1991) Viscous fluid flow, vol 3. McGraw-Hill, New York
  36. Wieselthaler GM, Schima H, Hiesmayr M, Pacher R, Laufer G, Noon GP, DeBakey M, Wolner E (2000) First clinical experience with the DeBakey VAD continuous-axial-flow pump for bridge to transplantation. *Circulation* 101:356–359
  37. Qian Y, Bertram CD (2000) Computational fluid dynamics analysis of hydrodynamic bearings of the VentrAssist rotary blood pump. *Artif Organs* 24:488–491
  38. Yano T, Sekine K, Mitoh A, Mitamura Y, Okamoto E, Kim DW, Nishimura I, Murabayashi S, Yozu R (2003) An estimation method of hemolysis within an axial flow blood pump by computational fluid dynamics analysis. *Artif Organs* 27:920–925



**Erfan Nammakie** was born in 1986 in Iran. He holds a bachelor's degree in mechanical heat and transfer from Islamic Azad University of Mashhad and a master's degree in biomedical engineering from Sahand University of Technology of Sahand, Tabriz. He has published one conference paper and two ISI papers.



**Dr. Hanieh Niroomand-Oscui** was born in 1974 in Iran. She did the Ph.D. in biomedical engineering in Amirkabir University of Technology degree in 2007. She is Associate professor of biomedical engineering since 2014. She teaches heat and mass transfer in biomedical engineering, biofluid mechanics, bioinstrumentation and artificial organs courses in Sahand University of Technology. Her research interests include cardiovascular biomechanics, fluid–solid interaction in biological systems, heat and mass transport in biological systems and artificial organs. She has published more than 35 conference papers, 15 ISI papers in the fields which are mentioned above.



**Mojtaba Koochaki** was born in 1986 in Iran. He holds a bachelor's degree in mechanical heat and transfer from Shiraz University and a master's degree in biomedical engineering from Sahand University of Technology of Sahand, Tabriz. He has published one conference paper and two ISI papers.



**Dr. Farzan Ghalichi** was born in Iran. He did the Ph.D. in the Mechanical Engineering Department with collaboration of the Surgery Department of the Laval University and Quebec Biomaterial Institute, and now he is professor of biomedical engineering. He teaches Computational Fluid Dynamics, Fluid Mechanics in Biological Systems and Finite Element Method in Biomechanics courses in Sahand University of Technology. His research interests include cardiovascular biomechanics, Solid and Fluid Mechanics, and Blood Flow Circulation System. He has published more than 65 conference papers and 25 ISI papers in the fields which are mentioned above.